Machine learning model predicts new-onset lower extremity deep vein thrombosis after pelvic fracture surgery and targeted diagnosis

Haoyuan Fu1,2*,Qi Dong,1,2*,Guoqiang LI1,2*, Kuo Zhao 1,2#， Zhiyong Hou 1,2#, Yingze Zhang 1,2#

1 Department of Orthopedic Surgery，Third Hospital of Hebei Medical University，Shijiazhuang，Hebei，China..

2Orthopaedic Research Institute of Hebei Province，Third Hospital of Hebei Medical University，Shijiazhuang，Hebei，China.

#Corresponding author: Dr. Zhiyong Hou，Address: Department of Orthopaedical Surgery，the Third Hospital of Hebei Medical University，Shijiazhuang 050051，China. Mail address: drzyhou@hebmu.edu.cn

Dr. Kuo Zhao, Address : Department of Orthopaedical Surgery，the Third Hospital of Hebei Medical University，Shijiazhuang 050051，China. Mail address: Surzhao@163.com

Abstract

Background: Postoperative new-onset deep vein thrombosis (PNO-DVT) of the lower extremities represents a prevalent and serious clinical complication following pelvic fractures, which substantially impedes patient rehabilitation and diminishes quality of life. Conventional risk assessment methodologies exhibit inherent limitations, rendering them inadequate for precise prediction and individualized management of DVT. In recent years, machine learning techniques have demonstrated significant advantages in data analysis, emerging as promising tools for predicting postoperative DVT risk. This study sought to investigate the predictive efficacy of machine learning models for the development of new-onset lower extremity deep vein thrombosis following pelvic fracture surgery.

Methods: Data from 745 patients who underwent pelvic fracture surgery at our hospital between January 2016 and December 2019 were collected. The analysis encompassed demographic information, general patient data, preoperative laboratory test results, surgical details, and scoring systems. Initially, the data were analyzed using univariate logistic regression, least absolute shrinkage and selection operator (LASSO) regression, and multivariate logistic regression to identify 12 independent risk factors, including age, HDL-C, and ApoB. Subsequently, the dataset was partitioned into a training set and a test set at a 7:3 ratio. Six models were employed for analysis, including logistic regression, support vector machine (SVM), random forest, XGBoost, LightGBM, and AdaBoost.

Conclusion: Comparative analysis of the six machine learning models revealed XGBoost exhibited the highest performance (AUC: 0.8633), followed by LightGBM (0.8349), random forest (0.8055), logistic regression (0.7503), SVM (0.7505), and AdaBoost (0.8179). Model sensitivity ranged from 0.3684 to 0.8421, and accuracy ranged from 0.6502 to 0.9238.

Keywords

DVT risk prediction; Machine learning; Model prediction; Postoperative complications

Background

Pelvic fractures represent a severe form of trauma associated with a broad spectrum of complex and diverse postoperative complications. Notably, the development of deep vein thrombosis (DVT) in the lower extremities is a critical factor contributing to elevated mortality and disability rates among these patients. Over the years, numerous studies have demonstrated that individuals with pelvic fractures are predisposed to a hypercoagulable state, attributed to factors such as prolonged immobilization, tissue damage, and postoperative inflammatory responses, thereby elevating the risk of DVT [1-2]. The incidence of lower limb DVT in patients with pelvic fractures has been reported to reach 20% or higher, with most cases occurring postoperatively, thereby significantly impacting patient rehabilitation outcomes and quality of life [3-4].

Traditional risk assessment for DVT predominantly relies on clinical experience and isolated clinical indicators, such as D-dimer levels, patient age, and body mass index, in conjunction with straightforward assessment scales, including the Wells score, Autar score, and Padua score. However, these methodologies exhibit notable limitations in practical application, characterized by inadequate predictive accuracy and specificity, impairing the ability to achieve early and precise risk stratification in clinical settings. For instance, while the Autar and Padua scores demonstrate high sensitivity in intensive care unit (ICU) populations, their low specificity contributes to a significant rate of misdiagnosis, thereby complicating the implementation of tailored preventive strategies[5-6]. Furthermore, there is a dearth of specialized risk assessment instruments for patients with pelvic fractures, as traditional models

are predominantly grounded in single disease contexts, failing to account for the intricate pathological conditions associated with pelvic fractures[2].

With the rapid advancement of artificial intelligence and machine learning, risk prediction models leveraging big data have demonstrated significant potential in the medical domain. Machine learning is adept at processing extensive, multidimensional clinical datasets, enabling automatic learning and identification of complex, nonlinear relationships, thereby enhancing the accuracy and stability of risk assessments. Recent studies have developed machine learning models to predict postoperative DVT risks in patients undergoing brain trauma, tumor surgeries, and multiple injuries, achieving commendable predictive performance. For instance, models utilizing algorithms such as Gradient Boosting Machine (GBM) and LightGBM have reported area under the curve (AUC) values of 0.85 or higher in predicting DVT following brain trauma and brain tumor surgeries, markedly outperforming traditional statistical models[7-9]. Furthermore, integrating feature selection via Support Vector Machine (SVM) with reinforcement learning algorithms has achieved an accuracy of 95.9% for DVT risk prediction, underscoring the distinct advantages of machine learning in extracting critical risk factors and optimizing prediction models [10].

Previous studies on pelvic fracture patients have sought to develop risk prediction models based on clinical variables. These include multifactorial regression models that integrate factors such as emergency abdominal surgery, the Injury Severity Score (ISS), and indicators of renal and liver function. The resulting risk assessment nomogram has demonstrated high predictive accuracy, with an AUC of approximately 0.88, in both training and validation cohorts, thereby serving as an effective tool for preoperative risk stratification of DVT[2]. Nonetheless, the comprehensive application of machine learning techniques to predict the risk of new-onset lower limb DVT following pelvic fracture surgery remains nascent. Accordingly,

there is a pressing need to systematically incorporate large-scale, multicenter datasets and integrate multimodal clinical information to develop a more precise, clinically valuable prediction model with substantial clinical application potential.

Accordingly, a combination of traditional logistic regression and machine learning algorithms was adopted in the present study to develop a predictive model for new-onset lower limb DVT after pelvic fracture surgery, thereby enhancing clinical decision-making.

Methods

Data collection and processing

The study collected data from 857 patients diagnosed with pelvic fractures at the Third Hospital of Hebei Medical University from January 2016 to December 2019. After excluding 112 patients with preoperative thrombosis, 745 patients who developed postoperative DVT were included in the final analysis. The incidence of postoperative non-occlusive deep vein thrombosis (PNO-DVT) was 8.5% (n=64/681), with a predominance of male patients (74.8%, n=558/857).

Identification of risk factors for PNO-DVT

Independent risk factors were identified using a two-step analytical approach. Initially, a single-factor logistic regression analysis was employed to select factors with a P-value ≤ 0.05. Subsequently, the least absolute shrinkage and selection operator (LASSO) regression was utilized to further refine the selection of influencing factors for postoperative thrombosis, addressing potential collinearity issues. In the LASSO regression model, an increasing λ value intensified the penalty term, driving the coefficients of the independent variables towards zero. This regularization process effectively mitigated model overfitting. Based on the nine variables identified through univariate analysis and LASSO regression, a multivariate logistic regression was conducted to identify independent predictors of postoperative thrombosis.

Model establishment

The dataset for model establishment was derived from selecting 12 significant features identified through single-factor analysis. This dataset was then randomly partitioned into a training set (70%) and a test set (30%). Given the approximately 1:10 ratio of positive to negative samples, a notable class imbalance was present. To mitigate potential model bias towards the negative samples, which could lead to a diminished recall rate, sampling techniques were applied exclusively to the training set, leaving the test set unaltered. Model evaluation was subsequently conducted to more accurately assess the predictive capabilities of the models. Six machine learning algorithms, including logistic regression, SVM, random forest, XGBoost, LightGBM, and AdaBoost, were employed to develop six distinct models.

All statistical analyses and data visualizations were executed using R version 4.5.1. The study utilized the "xgboost", "e1071", "randomForest", "rpart", and "caret" packages for machine learning modeling, and the "tidyverse", "pROC", "ggplot2", "gridExtra", "tibble", and "shapviz" packages for data organization and visualization.

Results

1. Results of univariate logistic regression analysis

According to the univariate analysis of baseline characteristics in Table 1, age, hypertension, kidney disease, rheumatoid disease, peripheral vascular disease, and body mass index (BMI) were identified as potential risk factors for the development of postoperative thrombosis.

The univariate logistic regression analysis of surgical and blood transfusion data (Table 2) identified several potential risk factors for postoperative thrombosis. These factors included surgical approach (fracture reduction), type of bone graft, duration of the operation, intraoperative blood loss, intraoperative blood transfusion, method of blood transfusion, and

131 the administration of suspended red blood cells, plasma, and cryoprecipitate coagulation
132 factors.

133 The results of the univariate logistic regression analysis, presented in Table 3 of the
134 preoperative laboratory data, indicated that Gamma-Glutamyl Transferase (GGT), High-
135 Density Lipoprotein Cholesterol (HDL-C), Apolipoprotein B (ApoB), Total Carbon Dioxide
136 (TCO2), Glucose (GLU), Glasgow Admission Prognostic Score (GAP), Eosinophil Count
137 (EOS), and Mean Platelet Volume (MPV) represented potential risk factors for postoperative
138 thrombosis.
139 Further analysis evaluated systemic inflammatory markers, including the Systemic Immune-
140 Inflammation Index (SII), Neutrophil-to-Lymphocyte Ratio (NLR), and Platelet-to-
141 Lymphocyte Ratio (PLR). However, none of these indicators demonstrated significant
142 differences, as presented in Table 4.

143 Table 4: Univariate Analysis of Validation Index Scores

variables	data type	OR(95%CI)	P
SII (plt*neut/lymph)	CV	1(1-1)	0.475
NLR (neut/lymph)	CV	0.991(0.943-1.04)	0.704
PLR (plt/lymph)	CV	0.998(0.996-1)	0.128

144

145 **2. LASSO regression for feature selection**

146 LASSO regression was employed to further identify the factors influencing postoperative
147 thrombosis. To mitigate collinearity in the data analysis, LASSO regression was used to select
148 variables with *P*-values < 0.05 from the univariate analysis. As λ increased, the penalty also
149 increased, leading to the gradual shrinkage of the regression coefficients of the independent
150 variables towards zero. This regularization term effectively reduced model overfitting. Figures

1 and 2 illustrate the variable selection process using LASSO regression and the impact of cross-validation on overfitting. In Figure 1, each curve represents the trajectory of a variable's coefficient, with the ordinate indicating the coefficient value and the abscissa showing the parameter λ, which controls the regularization intensity. As λ varied, the coefficients of the variables progressively approached zero, ultimately retaining only those variables with non-zero coefficients. Figure 1 demonstrates the determination of the optimal λ value via 10-fold cross-validation, indicated by a vertical dotted line. The left dotted line illustrated that when Lambda was set to Lambda.min, 18 variables were selected, whereas the right dotted line demonstrated that when Lambda was set to Lambda.1se, 13 variables were selected. In this study, Lambda.1se (i.e., Lambda = 0.01641399) was selected as the optimal penalty coefficient for the model. Following the LASSO regression analysis, variables with non-zero regression coefficients were identified, namely age, nephropathy, peripheral vascular disease, BMI, fracture reduction, operation time, intraoperative blood loss, de-erythrocytized RBC, HDL-C group, ApoB group, GLU group, GAP group, and MPV group, as presented in Table 5.

Figure 1: Feature selection process using Least Absolute Shrinkage and Selection Operator (LASSO) regression.

Figure 2: Graph of the Optimal λ Selection for Cross-Validation

Table 5: Lasso Result Coefficient Table

variables	**coefficient**

Age	0.1448
hypertension	0.0000
nephropathy	0.1127
rheumatoid disease	0.0000
peripheral vascular disease	0.1021
BMI	0.1217
fracture reduction	0.1159
Bone graft type	0.0000
time of operation	0.0492
Intraoperative blood loss	0.2299
Intraoperative blood transfusion	0.0000
Blood transfusion method	0.0000
red blood cells suspension	0.1791
Input plasma volume	0.0000
Cold precipitate coagulation factors	0.0000
GGT	0.0000
HDL-C	-0.1370
APOB	0.0610
TCO2	0.0000
GLU	0.0612
GAP	0.1014
E0S	0.0000
MPV	-0.0684

3.Multivariate Logistic Regression Analysis

Building on the nine variables identified through univariate analysis and LASSO regression, a multivariate logistic regression analysis was conducted to identify independent predictors of postoperative thrombosis. The assignment outcomes for the independent variables are presented in the table below. Our analysis identified age, nephropathy, BMI, fracture reduction,intraoperative blood loss, administration of red blood cell suspension, HDL-C, ApoB, GAP, and MPV as independent risk factors for blood transfusion. The detailed results of the regression analysis are presented in Table 6.

Table 6: Independent Predictors of Postoperative Thrombosis in Multivariate Logistic Regression Analysis

variables	β	standard	OR(95% CI)	P
Age	0.022	0.011	1.022(1.000-1.044)	0.046
nephropathy	2.519	0.923	12.415(2.033-75.826)	0.006
peripheral vascular disease	2.702	1.358	14.917(1.041-213.739)	0.047
BMI	0.092	0.043	1.096(1.007-1.193)	0.034
fracture reduction	1.859	0.851	6.420(1.210-34.065)	0.029
time of operation	0.001	0.002	1.001(0.998-1.004)	0.507
Intraoperative blood loss	0.000	0.0002	1.0005(1.0001-1.0010)	0.024
red blood cells suspension	0.000	0.0001	1.0003(1.0001-1.0005)	0.007
HDL-C < 0.9(Refer to 0.9-2)	-0.892	0.322	0.410(0.218-0.770)	0.006
APOB < 0.8((Refer to 0.8-1.2)	0.566	0.348	1.761(0.891-3.482)	0.104
APOB > 1.2((Refer to 0.8-1.2)	0.959	0.489	2.609(1.001-6.799)	0.050
GLU > 6.1(Refer to 3.9-6.1)	0.608	0.305	1.836(1.010-3.336)	0.046
GAP < 8((Refer to 8-16)	0.549	0.332	1.731(0.904-3.316)	0.098

GAP > 16(Refer to 8-16)	2.270	0.682	9.676(2.540-36.865)	0.001
MPV < 7.4(Refer to 7.4-11)	-0.977	0.478	0.376(0.147-0.961)	0.041
MPV > 11(Refer to 7.4-11)	-0.468	1.100	0.627(0.073-5.409)	0.671

Establishment and Analysis of Postoperative PNO-DVT Prediction Model Based on Machine Learning Algorithms

1. Establishment of the prediction model and performance evaluation

The twelve significant features identified from the preceding univariate analysis were selected as the dataset for the final model construction. The dataset was randomly split into a training set (70%) and a test set (30%). Given that the ratio of positive to negative samples was approximately 1:10, there was a notable imbalance. To mitigate the risk of the model being biased towards the negative samples during prediction, which could result in an unacceptably low recall rate, sampling was conducted on the training set; however, no processing was applied to the test set. This approach ensured that the model evaluation more accurately reflected the model's predictive capabilities. Six machine learning algorithms, including logistic regression, SVM, random forest, XGBoost, LightGBM, and AdaBoost, were employed to construct six distinct models. Among these, the XGBoost algorithm achieved the highest AUC value of 0.8633, indicating superior predictive performance for postoperative thrombosis within this dataset (Table 7). Consequently, XGBoost was determined to be the optimal model(Figure 3). Figure 4 illustrates the feature importance rankings for the random forest, XGBoost, LightGBM, and AdaBoost models.

Table 7: Performance Evaluation of Each Model's Prediction Model

Model Name	Accuracy	Sensitivity	Specificity	F1	AUC

logistic regression	0.6771	0.7368	0.6716	0.2800	0.7503
random forest	0.9238	0.3158	0.9804	0.4138	0.8055
XGBoost	0.8117	0.8421	0.8088	0.4324	0.8633
LightGBM	0.8879	0.3684	0.9363	0.3590	0.8349
SVM	0.6502	0.6842	0.6471	0.2500	0.7505
AdaBoost	0.9283	0.4211	0.9755	0.5000	0.8179

Figure 3: Comparison of ROC curves for each model

Figure 4: Model Feature Importance Chart

2. Explanatory analysis based on SHAP

Figures 4 and 5 provide visual representations of the feature importance rankings derived from SHAP values in the XGBoost model. Specifically, Figure 4 presents a swarm plot, while Figure 5 displays a feature importance plot. Both figures effectively illustrate the relative significance of each feature within the model. Age was identified as the most important predictor, followed by intraoperative blood loss, red blood cell suspension, BMI, GLU group, GAP group, reduction method group, MPV group, HDL-C group, ApoB group, kidney disease, and peripheral vascular disease(Figure 6).

Figure 5: Summary plot of SHAP (SHapley Additive exPlanations) values, illustrating the impact of the top features on the model's output

Figure 6: Feature Importance Ranking Chart Based on Shap Values

3.Analysis based on SHAP waterfall chart and force-directed layout

Figure 7 demonstrates the utility of SHAP force plots for deconstructing individual predictions. These visualizations elucidate the contribution of each feature to a single sample's outcome, where the color spectrum represents the direction of influence: features in yellow elevate the prediction score, while those in purple diminish it. The vertical axis enumerates the specific variables and their respective values for the given case. To illustrate this interpretability, force plots for representative positive and negative cases were generated. Analysis of a high-risk (positive) patient revealed that the model's prediction was predominantly driven by several key factors. The patient's age of 43 years was the most substantial contributor, increasing the prediction score by +0.269. This was closely followed by the administration of 2400 mL of packed red blood cells (+0.257) and an intraoperative blood loss of 700 mL (+0.16). Membership in GLU Group 1 provided a further, though smaller, positive influence (+0.103). Conversely, certain features moderated the overall risk. Membership in the GAP Group 0 exerted a slight protective effect (negative impact), partially offsetting the risk-enhancing factors. Other variables, such as HDL-C Group 0, MPV Group 0, reduction method 2, and ApoB Group 2, demonstrated minimal influence on the final prediction, despite their positive directional effect. The collective impact of the remaining features was negligible.

The values associated with the features of negative sample patients are detailed as follows: Age 35 exerted the most significant negative impact on the prediction value, decreasing it by 0.766. The administration of 400 units of red blood cell suspension reduced the prediction value by 0.21, indicating a notable inhibitory effect. A BMI of 25.0 contributed a negative impact of 0.159, further decreasing the prediction value. The MPV group value of 1 reduced the

prediction value by 0.0616, acting as a factor with a negative inhibitory effect. Conversely, the GLU group value of 1, highlighted in yellow, positively influenced the prediction value, albeit with a relatively small amplitude. Features such as the GAP group value of 0 and intraoperative blood loss of 600, marked in purple, negatively affected the prediction value, though their influence was relatively minor, as indicated by the figure. Besides, features such as the HDL-C group value of 1 and the reduction method value of 2 yielded a discernible impact on the prediction value, with the degree of influence being relatively small, as illustrated in the figure. The remaining 3 had a negligible impact on the prediction value.

Figure 7: The Case's Attempt

Discussion

In recent years, the application of machine learning technology in the medical domain has notably expanded, particularly in thrombosis risk prediction, where it has demonstrated considerable benefits. Machine learning models can predict the likelihood of DVT after fractures or surgery, creating novel opportunities for tailored prevention. Empirical studies have shown that machine learning algorithms are proficient at handling substantial volumes of high-dimensional data, thereby facilitating the identification of novel risk factors and enhancing patient risk stratification[11].

Machine learning models have demonstrated significant efficacy in predicting DVT following fractures. For example, a study developed several machine learning models to forecast the incidence of DVT after tibial fracture surgery. Notably, the random forest model, when integrated with recursive feature elimination (RFE), achieved an AUC of 0.99, indicating exceptionally high predictive accuracy [12]. Furthermore, the support vector machine model,

when combined with Boruta or LASSO feature selection methods, demonstrated superior calibration, underscoring the reliability of these models for risk estimation [12].

In various surgical contexts, machine learning models have shown significant promise in predicting DVT. For example, in the context of laparoscopic surgery, a study assessed 20 machine learning algorithms and developed a stacked model comprising the five most effective algorithms. This model outperformed the conventional Caprini score in external validation [13]. Besides, in the context of gastric cancer surgery, a machine learning model utilizing imaging data has emerged as an innovative non-invasive predictive tool, demonstrating enhanced efficacy in the early detection and management of DVT [14].

The use of machine learning to predict DVT extends beyond the postoperative context. In patients experiencing spontaneous intracerebral hemorrhage, machine learning algorithms have been employed to forecast the risk of lower extremity DVT during hospitalization. The Light Gradient Boosting Machine (LGBM) model was found to exhibit a notable advantage in DVT prediction[15]. Furthermore, in oncology patients undergoing chemotherapy, machine learning models are utilized to evaluate the risk of catheter-related thrombosis. Despite the clinical application being constrained by complexity, the Bayesian learning model offers a simplified and robust alternative[16].

As the utilization of machine learning algorithms in the medical field continues to expand, several researchers have endeavored to develop predictive models for DVT following fracture surgery using these advanced techniques. In the context of predicting DVT after various fractures or surgical procedures, numerous studies have demonstrated that machine learning models exhibit good performance in identifying significant risk factors and facilitating risk stratification. For instance, researchers have employed a range of algorithms for predicting DVT after knee and hip replacement surgeries, including XGBoost, RF, and SVM, integrating

288 patient electronic health records (EHRs) to construct a highly accurate predictive model,
289 achieving an AUC exceeding 0.92, which markedly surpasses the traditional Caprini score [17].
290 Similarly, in the prediction of DVT following spinal surgery, the combination of Boruta and
291 LASSO algorithms for feature selection enabled the random forest model to perform
292 exceptionally well, accurately identifying patients at high risk [18]. Furthermore, a study
293 investigating DVT following surgical intervention for lower limb fractures compared various
294 machine learning models, including XGBoost, Random Forest, and Logistic Regression. The
295 results revealed that XGBoost exhibited superior performance with an AUC of 0.979,
296 indicating robust predictive capability[19].

297 Machine learning models offer substantial advantages over logistic regression in the context of
298 large sample datasets, a perspective corroborated by numerous studies. Primarily, machine
299 learning techniques excel at handling high-dimensional data and handling missing values.
300 Contemporary machine learning approaches, including penalized regression, tree-based
301 models, and deep learning, exhibit good performance in handling missing data within high-
302 dimensional contexts, mitigating non-response bias, and demonstrating superiority in both
303 simulation studies and practical applications[20]. Furthermore, in the analysis of large-scale
304 neuroimaging datasets, machine learning effectively mitigates overfitting issues by integrating
305 the predictive strengths of multiple classifiers, thereby enhancing the model's generalization
306 capabilities[21].

307 In the medical domain, machine learning models have demonstrated superior performance
308 compared to traditional logistic regression models in predicting patient readmission and
309 mortality rates following colon cancer surgery. Empirical research indicates that models
310 developed using machine learning algorithms, such as Random Forest and XGBoost, exhibit
311 significantly higher AUC values than logistic regression models, thereby reflecting enhanced

312 discriminatory capabilities[22]. Similarly, in the context of risk stratification for COVID-19
313 patients, machine learning models achieve substantially higher AUC values compared to
314 logistic regression models, suggesting greater accuracy in identifying patients at risk of severe
315 outcomes [23].

316 Moreover, machine learning models demonstrate superior capabilities for handling the effects
317 of large-scale datasets and the intricate interactions among variables. Empirical studies have
318 shown that machine learning models exhibit greater robustness to variations in dataset size,
319 whereas deep learning models can maintain strong performance even in the absence of
320 interaction terms [24]. Another study demonstrated that machine learning models could enhance
321 the prediction of post-surgical complications by reliably identifying high-risk patients, yielding
322 more precise prognostic data[25].

323 In this study, six predictive models were developed, including a logistic regression model, to
324 predict PNO-DVT. The logistic regression model achieved an AUC of 0.7503, ranking fourth
325 in performance. Notably, the XGBoost model demonstrated the best performance
326 (AUC=0.8633).

327 In patients with pelvic fractures, the severity of vascular injury is significantly correlated with
328 prognosis. Research indicates that, even in cases of relatively isolated pelvic injuries, the
329 severity of vascular injury is more strongly associated with clinical outcomes than the
330 anatomical complexity of the fracture itself [26]. Such vascular injuries not only elevate the risk
331 of hemorrhage but may also initiate a series of inflammatory responses, thereby exacerbating
332 the hypercoagulable state of the blood. In clinical practice, the management of trauma stress
333 and inflammatory responses is crucial for improving the prognosis of patients with pelvic
334 fractures. Research has shown that chronic psychological and social stress can affect the
335 immune response through the β-adrenergic receptor signaling pathway, thereby influencing

336 fracture healing[26]. Therefore, interventions targeting traumatic stress and inflammatory
337 responses may alleviate hypercoagulability and improve overall patient prognosis.
338 Accordingly, systemic inflammatory indicators SII, NLR, and PLR were incorporated into our
339 analysis. Ultimately, none of these indicators were identified as significant predictors in this
340 patient population.

341 Subsequently, SHAP values were employed to elucidate the probability of PNO-DVT as
342 predicted by the XGBoost model. The analysis of SHAP values revealed that age was the most
343 significant factor, followed by intraoperative blood loss, leukocyte removal, BMI, GLU group,
344 GAP group, reduction method group, MPV group, HDL-C group, ApoB group, kidney disease,
345 and peripheral vascular disease. Age and BMI, recognized as common cardiovascular risk
346 factors, have been consistently associated with thrombosis in numerous studies. Current
347 evidence indicates that older patients are at an increased risk for thrombotic events, potentially
348 due to decreased vascular elasticity and the presence of atherosclerosis [28]. Furthermore, an
349 elevated BMI has been linked to metabolic syndrome and inflammatory responses, both of
350 which may contribute to the development of thrombosis [29].

351 Intraoperative blood loss and the volume of suspended red blood cells transfused
352 postoperatively are critical determinants influencing postoperative thrombosis. Significant
353 intraoperative blood loss can result in hemodynamic instability, whereas excessive
354 postoperative transfusion of suspended red blood cells may elevate blood viscosity, thereby
355 augmenting the risk of thrombosis [30]. These factors necessitate careful consideration in
356 postoperative management to mitigate the risk of thrombosis.

357 Among laboratory test indicators, MPV is recognized as a marker of platelet activation and is
358 closely associated with thrombosis. Empirical evidence suggests that patients with elevated
359 MPV are more susceptible to venous thromboembolism (VTE), potentially due to the increased

360 platelet volume, which enhances platelet reactivity and thus promotes thrombosis [31-32].
361 Furthermore, integrating MPV with other hematological indicators can enhance the accuracy
362 of thrombosis risk prediction [33].

363 Elevated glucose levels are significantly correlated with the incidence of DVT. Research
364 indicates that hyperglycemia elevates the risk of thrombosis, potentially due to increased blood
365 viscosity and vascular endothelial dysfunction associated with high glucose levels [34].
366 Furthermore, individuals with diabetes are predisposed to thrombosis as a result of prolonged
367 hyperglycemia, substantiating that glucose represents a risk factor for DVT [35].

368 Secondly, triglycerides and HDL-C are integral to lipid metabolism. Elevated triglyceride
369 levels and reduced HDL-C levels have been linked to the incidence of DVT. Research indicates
370 that dyslipidemia can damage the vascular endothelium and trigger inflammatory responses,
371 thereby elevating the risk of thrombosis [36-37]. Furthermore, low-density lipoprotein cholesterol
372 (LDL-C) and the lymphocyte-to-lymphocyte ratio (LLR) have been documented as predictors
373 of DVT, underscoring the significant role of lipid metabolism disorders in the pathogenesis of
374 DVT [37].

375 Apolipoprotein B (APOB), the primary component of low-density lipoprotein, is significantly
376 associated with atherosclerosis and thrombosis. Research indicates that elevated levels of
377 APOB may elevate the risk of deep vein thrombosis (DVT) by promoting lipid deposition
378 and vascular endothelial damage [38].

379 In conclusion, our machine learning model identified age, intraoperative blood loss,
380 intraoperative and postoperative blood transfusion, body mass index (BMI), glucose (GLU),
381 and mean platelet volume (MPV) as the most critical predictors of postoperative non-
382 occlusive deep vein thrombosis (PNO-DVT) in patients with pelvic fractures across the entire
383 dataset. The collection of these biomarkers facilitates the prediction of postoperative PNO-
384 DVT risk, thereby informing clinical practice. Furthermore, we employed SHapley Additive
385 exPlanations (SHAP) to enhance the model's interpretability. SHAP values assist clinicians in
386 providing personalized interventions for patients at high risk of DVT, allowing for tailored
387 intervention strategies based on individual patient risk factors rather than a standardized
388 treatment approach for all patients. This personalized approach promotes the efficient
389 allocation of medical resources.

390 Conclusion

391 In this study, we employed six models, including logistic regression, SVM, random forest,
392 XGBoost, LightGBM, and AdaBoost, to establish a predictive model for new-onset DVT
393 following pelvic fracture surgery. Among these machine learning models, XGBoost
394 demonstrated superior performance, achieving the highest AUC of 0.8633. The integration of
395 machine learning models into clinical practice has the potential to enhance the prognosis of
396 patients with pelvic fractures by facilitating efficient risk stratification for post-operative new-
397 onset DVT.

398 ## Abbreviations

399 PNO-DVT postoperative new-onset deep venous thrombosis

400 DVT deep venous thrombosis

401 CV continuous variable

402 ## Declarations

403 ***Ethics approval and consent to participate***

404 According to the Helsinki Declaration, this study has been approved by the Ethics Committee
405 of the Third Hospital of Hebei Medical University. Before analysis, all data were anonymized,
406 and since it was a retrospective study design, obtaining patient consent was not necessary.

407 ***Consent for publication***

408 All the authors have agreed to publish.

409 ***Availability of data and materials***

410 Data cannot be published without patients' consent. Researchers who are interested for
411 academic need could contact the corresponding authors.

412 ***Competing interests***

413 The authors declare that they have no competing interests.

414 ***Funding***

This study was supported by Key R&D Program of the China Ministry of Science and Technology (2024YFC2510600) and National Natural Science Foundation of China / 8220090241

Acknowledgements

Not applicable

Clinical trial number

Not applicable

Authors' information

Haoyuan Fu:fuhaoyuan2001@163.com;QiDong: 15755819518@163.com;Guoqiang Li: drgqli@outlook.com;Kuo Zhao: Surzhao@163.com; Zhiyong Hou: drzyhou@hebmu.edu.cn

1 Department of Orthopedic Surgery，Third Hospital of Hebei Medical University，Shijiazhuang，Hebei，China..

2Orthopaedic Research Institute of Hebei Province，Third Hospital of Hebei Medical University，Shijiazhuang，Hebei，China.

#Corresponding author: Dr. Zhiyong Hou，Address: Department of Orthopaedical Surgery，the Third Hospital of Hebei Medical University，Shijiazhuang 050051，China. Mail address: drzyhou@hebmu.edu.cn

Dr. Kuo Zhao, Address : Department of Orthopaedical Surgery，the Third Hospital of Hebei Medical University，Shijiazhuang 050051，China. Mail address: Surzhao@163.com

References

[1]. Chen H, Sun L, Kong X. Risk assessment scales to predict risk of lower extremity deep vein thrombosis among multiple trauma patients: a prospective cohort study. BMC Emerg Med. 2023 Dec 5;23(1):144. doi: 10.1186/s12873-023-00914-7. PMID: 38053029; PMCID: PMC10696745.

[2]. Chen Y, He J, Pan X. Prediction of risk factors for preoperative deep vein thrombosis in patients with pelvic fracture. Front Surg. 2025 Apr 28;12:1585460. doi: 10.3389/fsurg.2025.1585460. PMID: 40356946; PMCID: PMC12066781.

[3]. Wang H, Wu G, Chen CY, Qiu YY, Xie Y. Percutaneous screw fixation assisted by hollow pedicle finder for superior pubic ramus fractures. BMC Surg. 2022 Jun 3;22(1):216. doi: 10.1186/s12893-022-01659-z. PMID: 35658934; PMCID: PMC9166495.

[4]. Yang CS, Tan Z. Construction and validation of a predictive model for preoperative lower extremity deep vein thrombosis risk in elderly hip fracture patients: An observational study. Medicine (Baltimore). 2024 Sep 20;103(38):e39825. doi: 10.1097/MD.0000000000039825. PMID: 39312315; PMCID: PMC11419451.

[5]. Orak F, Saadat M, Saki Malehi A, Behdarvandan A, Esfandiarpour F. Comparison of the Pauda and the Autar DVT Risk Assessment Scales in Prediction of Venous Thromboembolism in ICU Patients. Med J Islam Repub Iran. 2024 Apr 30;38:48. doi: 10.47176/mjiri.38.48. PMID: 39399622; PMCID: PMC11469705.

[6]. Shekarchian S, Notten P, Barbati ME, Van Laanen J, Piao L, Nieman F, Razavi MK, Lao M, Mees B, Jalaie H. Development of a prediction model for deep vein thrombosis in a retrospective cohort of patients with suspected deep vein thrombosis in primary care.

J Vasc Surg Venous Lymphat Disord. 2022 Sep;10(5):1028-1036.e3. doi: 10.1016/j.jvsv.2022.04.009. Epub 2022 May 27. PMID: 35644336.

[7]. Tang Z, Li N, Tian Y. A nomogram for predicting risk factors for lower limb deep venous thrombosis in elderly postoperative patients with severe traumatic brain injury in the intensive care unit. Phlebology. 2025 Jul;40(6):446-455. doi: 10.1177/02683555251332988. Epub 2025 Apr 10. PMID: 40205921.

[8]. Wu L, Zhao Y, Yao G, Li X, Zhao X. Prediction and Analysis of Risk Factors for Lower Extremity Deep Vein Thrombosis After Craniotomy in Patients with Primary Brain Tumors: A Machine Learning Approach. Turk Neurosurg. 2025;35(4):636-643. doi: 10.5137/1019-5149.JTN.47938-24.3. PMID: 40577511.

[9]. Qiu W, Cui P, Li S, Tang Z, Chen J, Wang J, Li Y. Machine learning models predict risk of lower extremity deep vein thrombosis in hospitalized patients with spontaneous intracerebral hemorrhage. Sci Rep. 2025 Jul 10;15(1):24932. doi: 10.1038/s41598-025-10905-2. PMID: 40640445; PMCID: PMC12246041.

[10]. Li R, Chen S, Xia J, Zhou H, Shen Q, Li Q, Dong Q. Predictive modeling of deep vein thrombosis risk in hospitalized patients: A Q-learning enhanced feature selection model. Comput Biol Med. 2024 Jun;175:108447. doi: 10.1016/j.compbiomed.2024.108447. Epub 2024 Apr 12. PMID: 38691912.

[11]. Chrysafi P, Lam B, Carton S, Patell R. From Code to Clots: Applying Machine Learning to Clinical Aspects of Venous Thromboembolism Prevention, Diagnosis, and Management. Hamostaseologie. 2024 Dec;44(6):429-445. doi: 10.1055/a-2415-8408. Epub 2024 Dec 10. PMID: 39657652.

[12]. Baki H, Özçelik İB. Machine Learning-Based Prediction of Postoperative Deep Vein Thrombosis Following Tibial Fracture Surgery. Diagnostics (Basel). 2025 Jul

482 16;15(14):1787. doi: 10.3390/diagnostics15141787. PMID: 40722536; PMCID:
483 PMC12293441.
484 [13]. Yang SZ, Peng MH, Lin Q, Guan SW, Zhang KL, Yu HB. A machine learning-based
485 predictive model for the occurrence of lower extremity deep vein thrombosis after
486 laparoscopic surgery in abdominal surgery. Front Surg. 2025 May 30;12:1502944. doi:
487 10.3389/fsurg.2025.1502944. PMID: 40520687; PMCID: PMC12162540.
488 [14]. Zeng Y, Chen Y, Zhu D, Xu J, Zhang X, Ying H, Song X, Zhou R, Wang Y, Yu F.
489 Machine learning assisted radiomics in predicting postoperative occurrence of deep
490 venous thrombosis in patients with gastric cancer. BMC Cancer. 2025 Feb 7;25(1):220.
491 doi: 10.1186/s12885-025-13630-1. PMID: 39920636; PMCID: PMC11806839.
492 [15]. Qiu W, Cui P, Li S, Tang Z, Chen J, Wang J, Li Y. Machine learning models predict risk
493 of lower extremity deep vein thrombosis in hospitalized patients with spontaneous
494 intracerebral hemorrhage. Sci Rep. 2025 Jul 10;15(1):24932. doi: 10.1038/s41598-025-
495 10905-2. PMID: 40640445; PMCID: PMC12246041.
496 [16]. An T, Han H, Xie J, Wang Y, Zhao Y, Jia H, Wang Y. Enhancing prediction and
497 stratifying risk: machine learning and bayesian-learning models for catheter-related
498 thrombosis in chemotherapy patients. BMC Cancer. 2025 Mar 27;25(1):552. doi:
499 10.1186/s12885-025-13946-y. PMID: 40148861; PMCID: PMC11948715.
500 [17]. Wang X, Xi H, Geng X, Li Y, Zhao M, Li F, Li Z, Ji H, Tian H. Artificial Intelligence-
501 Based Prediction of Lower Extremity Deep Vein Thrombosis Risk After Knee/Hip
502 Arthroplasty. Clin Appl Thromb Hemost. 2023 Jan-Dec;29:10760296221139263. doi:
503 10.1177/10760296221139263. PMID: 36596268; PMCID: PMC9830569.
504 [18]. Wu X, Wang Z, Zheng L, Yang Y, Shi W, Wang J, Liu D, Zhang Y. Construction and
505 verification of a machine learning-based prediction model of deep vein thrombosis

formation after spinal surgery. Int J Med Inform. 2024 Dec;192:105609. doi: 10.1016/j.ijmedinf.2024.105609. Epub 2024 Aug 30. PMID: 39260049.

[19]. Wei C, Wang J, Yu P, Li A, Xiong Z, Yuan Z, Yu L, Luo J. Comparison of different machine learning classification models for predicting deep vein thrombosis in lower extremity fractures. Sci Rep. 2024 Mar 22;14(1):6901. doi: 10.1038/s41598-024-57711-w. PMID: 38519523; PMCID: PMC10960026.

[20]. Chen S, Xu C. Handling high-dimensional data with missing values by modern machine learning techniques. J Appl Stat. 2022 May 1;50(3):786-804. doi: 10.1080/02664763.2022.2068514. PMID: 36819079; PMCID: PMC9930810.

[21]. Lanka P, Rangaprakash D, Dretsch MN, Katz JS, Denney TS Jr, Deshpande G. Supervised machine learning for diagnostic classification from large-scale neuroimaging datasets. Brain Imaging Behav. 2020 Dec;14(6):2378-2416. doi: 10.1007/s11682-019-00191-8. PMID: 31691160; PMCID: PMC7198352.

[22]. Leonard G, South C, Balentine C, Porembka M, Mansour J, Wang S, Yopp A, Polanco P, Zeh H, Augustine M. Machine Learning Improves Prediction Over Logistic Regression on Resected Colon Cancer Patients. J Surg Res. 2022 Jul;275:181-193. doi: 10.1016/j.jss.2022.01.012. Epub 2022 Mar 11. PMID: 35287027.

[23]. Ye J, Hua M, Zhu F. Machine Learning Algorithms are Superior to Conventional Regression Models in Predicting Risk Stratification of COVID-19 Patients. Risk Manag Healthc Policy. 2021 Jul 29;14:3159-3166. doi: 10.2147/RMHP.S318265. PMID: 34349576; PMCID: PMC8328384.

[24]. Bailly A, Blanc C, Francis É, Guillotin T, Jamal F, Wakim B, Roy P. Effects of dataset size and interactions on the prediction performance of logistic regression and deep learning models. Comput Methods Programs Biomed. 2022 Jan;213:106504. doi: 10.1016/j.cmpb.2021.106504. Epub 2021 Oct 28. PMID: 34798408.

531 [25]. Michelsen C, Jørgensen CC, Heltberg M, Jensen MH, Lucchetti A, Petersen PB,
532 Petersen T, Kehlet H; Center for Fast-track Hip Knee Replacement Collaborative group;
533 Madsen F, Hansen TB, Gromov K, Jakobsen T, Varnum C, Overgaard S, Rathsach M,
534 Hansen L. Machine-learning vs. logistic regression for preoperative prediction of
535 medical morbidity after fast-track hip and knee arthroplasty-a comparative study. BMC
536 Anesthesiol. 2023 Nov 29;23(1):391. doi: 10.1186/s12871-023-02354-z. PMID:
537 38030979; PMCID: PMC10685559.
538 [26]. Wu YT, Cheng CT, Tee YS, Fu CY, Liao CH, Hsieh CH. Pelvic injury prognosis is
539 more closely related to vascular injury severity than anatomical fracture complexity: the
540 WSES classification for pelvic trauma makes sense. World J Emerg Surg. 2020 Aug
541 17;15(1):48. doi: 10.1186/s13017-020-00328-x. PMID: 32807185; PMCID:
542 PMC7433075.
543 [27]. Haffner-Luntzer M, Foertsch S, Fischer V, Prystaz K, Tschaffon M, Mödinger Y,
544 Bahney CS, Marcucio RS, Miclau T, Ignatius A, Reber SO. Chronic psychosocial stress
545 compromises the immune response and endochondral ossification during bone fracture
546 healing via β-AR signaling. Proc Natl Acad Sci U S A. 2019 Apr 23;116(17):8615-8622.
547 doi: 10.1073/pnas.1819218116. Epub 2019 Apr 4. PMID: 30948630; PMCID:
548 PMC6486758.
549 [28]. Rong X, Jiang L, Qu M, Yang S, Wang K, Jiang L. Risk factors and characteristics of
550 ischemic stroke in patients with immune thrombocytopenia: A retrospective cohort
551 study. J Stroke Cerebrovasc Dis. 2022 Oct;31(10):106693. doi:
552 10.1016/j.jstrokecerebrovasdis.2022.106693. Epub 2022 Aug 31. PMID: 36054971.
553 [29]. Hansen ES, Edvardsen MS, Aukrust P, Ueland T, Hansen JB, Brækkan SK, Morelli VM.
554 Combined effect of high factor VIII levels and high mean platelet volume on the risk of

555 future incident venous thromboembolism. J Thromb Haemost. 2023 Oct;21(10):2844-
556 2853. doi: 10.1016/j.jtha.2023.06.022. Epub 2023 Jun 29. PMID: 37393000.
557 [30]. Zhang YM, Chen W, Wei HL, Tang XH, Xie FH, Wang RX. Analysis of predictive
558 factors of thrombosis in autogenous arteriovenous fistula. J Vasc Access. 2024
559 Jul;25(4):1134-1139. doi: 10.1177/11297298221151135. Epub 2023 Jan 27. PMID:
560 36707987.
561 [31]. Edvardsen MS, Hansen ES, Hindberg K, Morelli VM, Ueland T, Aukrust P, Brækkan
562 SK, Evensen LH, Hansen JB. Combined effects of plasma von Willebrand factor and
563 platelet measures on the risk of incident venous thromboembolism. Blood. 2021 Dec
564 2;138(22):2269-2277. doi: 10.1182/blood.2021011494. PMID: 34161566.
565 [32]. Wang Z, Chen X, Wu J, Zhou Q, Liu H, Wu Y, Liu S, Liu Y. Low Mean Platelet
566 Volume is Associated with Deep Vein Thrombosis in Older Patients with Hip Fracture.
567 Clin Appl Thromb Hemost. 2022 Jan-Dec;28:10760296221078837. doi:
568 10.1177/10760296221078837. PMID: 35157546; PMCID: PMC8848069.
569 [33]. Jakobsen L, Frischmuth T, Brækkan SK, Hansen JB, Morelli VM. Joint Effect of
570 Multiple Prothrombotic Genotypes and Mean Platelet Volume on the Risk of Incident
571 Venous Thromboembolism. Thromb Haemost. 2022 Nov;122(11):1911-1920. doi:
572 10.1055/a-1863-2052. Epub 2022 May 26. PMID: 35617954.
573 [34]. Liu X, Li T, Xu H, Wang C, Ma X, Huang H, Hu Y, Chu H. Hyperglycemia may
574 increase deep vein thrombosis in trauma patients with lower limb fracture. Front
575 Cardiovasc Med. 2022 Sep 8;9:944506. doi: 10.3389/fcvm.2022.944506. PMID:
576 36158801; PMCID: PMC9498976.
577 [35]. Hang L, Haibier A, Kayierhan A, Abudurexiti T. Risk factors for deep vein thrombosis
578 of the lower extremity after total hip arthroplasty. BMC Surg. 2024 Sep 11;24(1):256.
579 doi: 10.1186/s12893-024-02561-6. PMID: 39261801; PMCID: PMC11389418.

[36]. Abdelmalik BHA, Leslom MMA, Gameraddin M, Alshammari QT, Hussien R, Alyami MH, Salih M, Yousef M, Yousif E. Assessment of Lower Limb Deep Vein Thrombosis: Characterization and Associated Risk Factors Using Triplex Doppler Imaging. Vasc Health Risk Manag. 2023 May 4;19:279-287. doi: 10.2147/VHRM.S409253. PMID: 37168880; PMCID: PMC10166097.

[37]. Guo H, Li C, Wu H, Ma M, Zhu R, Wang M, Yang B, Pan N, Zhu Y, Wang J. Low-density lipoprotein cholesterol-to-lymphocyte count ratio (LLR) is a promising novel predictor of postoperative new-onset deep vein thrombosis following open wedge high tibial osteotomy: a propensity score-matched analysis. Thromb J. 2024 Jul 16;22(1):64. doi: 10.1186/s12959-024-00635-2. PMID: 39014396; PMCID: PMC11250942.

[38]. Gu H, Yang F, Xie H, Li M, Wang Z, Sheng L. Serum VEGF, P-Selectin, HDL-C, Platelet Index, and Coagulation Function Index in Deep Vein Thrombosis after Traumatic Fracture. Clin Lab. 2024 Feb 1;70(2). doi: 10.7754/Clin.Lab.2023.230425. PMID: 38345981.

Table 1: Univariate Analysis of General Information

variables	targeted value	OR(95%CI)	P
age	CV	1.03(1.012-1.048)	0.001
hypertension	NO	Ref.	
	YES	2.029(1.055-3.903)	0.034

diabetes	NO	Ref.	
	YES	1.09(0.564-2.105)	0.798
cerebrovascular disease	NO	Ref.	
	YES	1.395(0.572-3.402)	0.464
cardiopathy	NO	Ref.	
	YES	1.128(0.389-3.268)	0.824
arrhythmia	NO	Ref.	
	YES	0.475(0.063-3.586)	0.471
respiratory failure	NO	Ref.	
	YES	0(0-Inf)	0.986
COPD	NO	Ref.	
	YES	0(0-Inf)	0.989
history of lung disease	NO	Ref.	
	YES	0(0-Inf)	0.987
pneumonia	NO	Ref.	
	YES	0(0-Inf)	0.986
spinal cord injury	NO	Ref.	
	YES	0(0-Inf)	0.986
tumour	NO	Ref.	
	YES	0(0-Inf)	0.984
cerebral trauma	NO	Ref.	
	YES	1.16(0.4-3.366)	0.784
hepatopathy	NO	Ref.	
	YES	0.936(0.279-3.136)	0.915

nephropathy	NO	Ref.	
	YES	6.649(1.552-28.493)	0.011
hyperthyroidism	NO	Ref.	
	YES	0(0-Inf)	0.989
rheumatoid disease	NO	Ref.	
	YES	10.952(1.516-79.096)	0.018
peripheral vascular disease	NO	Ref.	
	YES	21.935(1.961-245.341)	0.012
anemia	NO	Ref.	
	YES	0(0-Inf)	0.986
urinary tract infection	NO	Ref.	
	YES	0(0-Inf)	0.982
Surgical history	NO	Ref.	
	YES	0.688(0.359-1.32)	0.261
Paraplegia or quadriplegia	NO	Ref.	
	YES	4.361(0.829-22.945)	0.082
allergy	NO	Ref.	
	YES	1.265(0.638-2.507)	0.501
blood type	A	Ref.	
	B	1.529(0.744-3.144)	0.248
	AB	1.433(0.664-3.092)	0.359
	0	1.955(0.787-4.854)	0.149
Rh-negative Blood type	NO	Ref.	
	YES	0(0-Inf)	0.988

place of residence	County	Ref.	
	City	0.772(0.41-1.455)	0.424
Hospitalization season	spring	Ref.	
	summer	1.066(0.554-2.052)	0.849
	fall	0.714(0.344-1.482)	0.366
	winter	0.563(0.262-1.209)	0.141
Surgical season	spring	Ref.	
	summer	1.006(0.515-1.964)	0.987
	fall	0.852(0.419-1.733)	0.659
	winter	0.61(0.282-1.321)	0.210
Interval between admission and surgery	CV	0.987(0.942-1.036)	0.601
Total number of fractures	CV	1.053(0.93-1.193)	0.413
Cause of injury	1	Ref.	
	2	2.132(0.538-8.445)	0.281
	3	1.38(0.651-2.923)	0.401
	4	1.953(0.898-4.247)	0.091
	6	0(0-Inf)	0.981
Type of injury	closed injury	Ref.	
	open injury	1.353(0.663-2.76)	0.406
smoking history	NO	Ref.	
	YES	0.872(0.462-1.646)	0.673
Alcohol consumption history	NO	Ref.	
	YES	0.536(0.21-1.37)	0.193
height	CV	0.985(0.951-1.02)	0.387

weight	CV	1.014(0.994-1.036)	0.176
BMI	CV	1.104(1.027-1.186)	0.007

Cause of injury (1 = Simple fall, 2 = Injury from electric bike or bicycle, 3 = Car accident injury, 4 = Injury from falling from a height, 5 = Injury from sharp objects, 6 = Other injuries)

Table 2: Univariate Analysis of Surgical and Blood Transfusion Information

variables	**targeted value**	**OR(95%CI)**	**P**
	0	Ref.	
	1	1513860.09(0-Inf)	0.995

	2	1043423.998(0-Inf)	0.995
	3	1(0-Inf)	1.000
anesthesia method	1	Ref.	
	2	0.705(0.166-2.992)	0.636
	3	0.859(0.354-2.085)	0.737
Anesthesia group	1	Ref.	
	2	0.979(0.468-2.046)	0.954
fracture reduction	1	Ref.	
	2	5.715(1.377-23.717)	0.016
fixed form	1	Ref.	
	2	0.302(0.041-2.24)	0.241
	3	0(0-Inf)	0.989
internal fixator	0	Ref.	
	1	2.841(0.376-21.487)	0.312
	2	4.138(0.436-39.26)	0.216
	3	1.905(0.204-17.786)	0.572

	4	4.118(0.52-32.607)	0.180
	5	0(0-Inf)	0.991
	6	0(0-Inf)	0.992
	7	0(0-Inf)	0.992
	8	2.386(0.282-20.2)	0.425
bone grafting	NO	Ref.	
	YES	1.905(0.711-5.106)	0.200
Bone graft type	0	Ref.	
	1	8.288(1.812-37.914)	0.006
	2	0.884(0.204-3.825)	0.869
time of operation	CV	1.004(1.002-1.007)	<0.001
Intraoperative blood loss	CV	1.001(1-1.001)	<0.001
ASA	1	Ref.	
	2	0.747(0.345-1.616)	0.459
	3	0.871(0.378-2.01)	0.747
	4	1.083(0.121-9.684)	0.943

Intraoperative blood transfusion	CV	1(1-1.001)	0.008
Blood transfusion method	0	Ref.	
	1	1.35(0.382-4.772)	0.641
	2	1.895(1.059-3.391)	0.031
	3	2.181(0.95-5.005)	0.066
Surgery timing	1	Ref.	
	2	0.816(0.105-6.338)	0.846
Input suspended red blood cells	CV	1(1-1.001)	<0.001
The total volume of blood transfused	CV	0.97(0.046-20.657)	0.984
The amount of plasma transfused	CV	1.001(1-1.001)	0.009
The amount of platelets transfused	0	Ref.	
	1	1.417(0.317-6.34)	0.648
	2	0(0-Inf)	0.981
Albumin supplements	0	Ref.	
	1	1.243(0.686-2.254)	0.474

Anesthesia method 1 = Local anesthesia (including brachial plexus, cervical plexus nerve block) 2 = Spinal anesthesia (including intradural, extradural anesthesia, and combined spinal-epidural anesthesia) 3 = General

anesthesia; Anesthesia grouping: 1 local anesthesia; 2 general anesthesia; Reduction method 1 = Closed reduction 2 = Open reduction (or approach); Fixation method 1 = Internal fixation 2 = External fixation 3 = Conservative; Internal fixation device 0 = None 1 = Plate 2 = Intramedullary nail 3 = Kirschner wire 4 = Simple screw 5 = Total hip prosthesis 6 = Semi-hip prosthesis 7 = Rivet 8 = Others; Bone graft type 0 = No bone grafting 1 = Autologous bone 2 = Allogeneic bone; Blood transfusion method 0 = No blood transfusion 1 = Autologous blood transfusion 2 = Allogeneic blood transfusion 3 = Autologous + allogeneic blood transfusion; Surgery timing 1 = Daytime surgery 2 = Nighttime surgery

Table 3: Univariate Analysis of Laboratory Information

variables	**targeted**	**OR(95%CI)**	**P**
TP(g/L)	≥65	Ref.	
	< 65	1.178(0.697-1.991)	0.540

ALB(references 30–50 g/L)	30-50	Ref.	
	< 30 or > 50	1.305(0.769-2.212)	0.324
GLOB(references 20–40 g/L)	20-40	Ref.	
	< 20 or > 40	0.832(0.423-1.635)	0.593
A/G(references 1.2–2.4)	1.2-2.4	Ref.	
	< 1.2	0.588(0.293-1.182)	0.136
	> 2.4		0.980
ALT(references 9–50 U/L)	9-50	Ref.	
	< 9 or > 50	1.438(0.857-2.415)	0.169
AST(references 15–40 U/L)	15-40	Ref.	
	< 15 or > 40	1.632(0.974-2.733)	0.063
TBIL（references 1.7-17.1μmol/L）	1.7-17.1	Ref.	
	> 17.1	0.872(0.477-1.593)	0.655
DBIL (references 0-6.8 μmol/L)	0-6.8	Ref.	
	> 6.8	1.115(0.666-1.865)	0.679
IBIL (references1.7-10.2μmoL/L)	1.7-10.2	Ref.	
	> 10.2	0.859(0.47-1.569)	0.620
ALP(references 45–125 U/L)	45-125	Ref.	
	< 45	1.143(0.553-2.363)	0.719
	> 125	1.667(0.887-3.133)	0.113
GGT(references 10–60 U/L)	10-60	Ref.	
	< 10 or > 60	1.693(1.001-2.864)	0.050
CHE(references 5–12 U/L)	5-12	Ref.	
	< 5 or > 12	0.728(0.416-1.272)	0.265

TBA(references 1–10 μmol/L)	1-10	Ref.	
	< 1 or > 10	1.426(0.62-3.279)	0.404
HCRP(references 0-3mg/L)	≤3	Ref.	
	> 3	1.842(0.776-4.375)	0.166
LDH(references 0-250 U/L)	< 250	Ref.	
	≥250	1.421(0.825-2.448)	0.205
TC(references 0-5.2mmol/L)	≤5.2	Ref.	
	> 5.2	0(0-Inf)	0.981
TG(references 0-1.7mmol/L)	≤1.7	Ref.	
	> 1.7	0.823(0.395-1.712)	0.601
HDL-C(references 0.9-2mmol/L)	0.9-2	Ref.	
	< 0.9 or > 2	0.582(0.347-0.975)	0.040
LDL-C(references0-3.1mmol/L)	≤3.1	Ref.	
	> 3.1	0.777(0.301-2.002)	0.601
VLDL(references2-30mg/dL)	2-30	Ref.	
	< 2 or > 30	0.888(0.426-1.85)	0.751
APOB（references 0.8-1.2g/L）	0.8-1.2	Ref.	
	< 0.8	1.3(0.722-2.341)	0.381
	> 1.2	2.823(1.229-6.484)	0.014
Na+(references 137–147 mmol/L	137-147	Ref.	
	< 137	0.936(0.559-1.569)	0.803
	> 147	2.597(0.281-23.96)	0.400
K+(references 3.5–5.3 mmol/L)	3.5-5.3	Ref.	
	< 3.5	2.517(0.781-8.109)	0.122

	> 5.3	0.947(0.55-1.631)	0.844
CL-(references 99–110 mmol/L)	99-110	Ref.	
	< 99	1.13(0.604-2.116)	0.701
	> 110	2.153(0.709-6.54)	0.176
TCO2(references 20–30 mmol/L)	20-30	Ref.	
	< 20	3.289(1.49-7.258)	0.003
	> 30	0(0-Inf)	0.984
GLU(references3.9-6.1mmol/L)	< 6.1	Ref.	
	> 6.1	1.797(1.072-3.014)	0.026
CREA(references 57–97 mmol/L)	57-97	Ref.	
	< 57	1.062(0.484-2.333)	0.880
	> 97	1.411(0.703-2.833)	0.333
GAP(references 8-16 mmol/L)	8-16	Ref.	
	< 8	1.216(0.696-2.123)	0.492
	> 16	6.754(2.155-21.165)	0.001
UA(references 208–428 mmol/L)	208-428	Ref.	
	< 208	0.752(0.424-1.331)	0.328
	> 428	1.003(0.406-2.473)	0.995
CA(references 2.11–2.52 mmol/L)	2.11-2.52	Ref.	
	< 2.11	1.1(0.658-1.836)	0.717
	> 2.52	0(0-Inf)	0.985
P(references 0.85–1.51 mmol/L)	0.85-1.51	Ref.	
	< 0 . 85	0.207(0.028-1.531)	0.123
	> 1.51	1.114(0.51-2.432)	0.787

Mg(references 0.75–1.02 mmol/L)	0.75-1.02	Ref.	
	< 0.75	1.581(0.81-3.087)	0.180
	> 1.02	1.091(0.249-4.79)	0.908
WBC(references 3.5–9.5 × 109/L)	3.5-9.5	Ref.	
	< 3.5 or > 9.5	1.113(0.664-1.865)	0.684
NEUT(references 2.8–6.3 × 109/L)	2.8-6.3	Ref.	
	< 2.8 or > 6.3	0.907(0.534-1.541)	0.718
LYM(references 1.1–3.2 × 109/L)	1.1-3.2	Ref.	
	< 1.1 or > 3.2	1.177(0.544-2.544)	0.679
MON(references 0.1–0.6 × 109/L)	0.1-0.6	Ref.	
	< 0.1	0(0-Inf)	0.989
	> 0.6	0.989(0.532-1.839)	0.973
EOS(references 0.02–0.05 × 109/L)	0.02-0.05	Ref.	
	< 0.02	1.869(1.057-3.307)	0.032
	> 0.05	0(0-Inf)	0.987
BAS	> 0.06	Ref.	
	≤0.06	1.065(0.134-8.456)	0.952
NEUT(references 45–75%)	45-75	Ref.	
	< 45 or > 75	1.224(0.7-2.141)	0.479
LYM%references 20–40%	20-40	Ref.	
	< 20	0.948(0.563-1.597)	0.841
	> 40	2.625(0.286-24.117)	0.394
MON%(references 3–10%)	3-10	Ref.	
	< 3 or > 10	1.303(0.703-2.413)	0.401

E0S(references 0.02–0.05 × 109/L)	0.02-0.05	Ref.	
	< 0.02	1.869(1.057-3.307)	0.032
	> 0.05	0(0-Inf)	0.987
RBC	normal	Ref.	
	abnormal	1.569(0.697-3.53)	0.277
HGB(references > 110/120g/L)	normal	Ref.	
	abnormal	2.013(0.898-4.513)	0.089
HCT(references 40-50%)	40-50	Ref.	
	< 40	1.276(0.565-2.884)	0.558
	> 50	0(0-Inf)	0.985
MCV(references 82–100 fL)	82-100	Ref.	
	< 82	1.571(0.348-7.087)	0.556
	> 100	1.375(0.522-3.622)	0.519
MCH(references 27–34 pg)	27-34	Ref.	
	< 27	1.819(0.397-8.324)	0.441
	> 34	1.213(0.417-3.526)	0.723
MCHC(references 316–354 g/L)	316-354	Ref.	
	< 316	3.083(0.836-11.375)	0.091
	> 354	1.528(0.577-4.042)	0.394
RDW(references 11.6–16.5%)	11.6–16.5	Ref.	
	< 11.6	0.556(0.073-4.23)	0.571
	> 16.5	1.078(0.413-2.813)	0.877
PLT(references 125–350 × 10^9/L)	125-350	Ref.	
	< 125	0.577(0.174-1.915)	0.369

	> 350	0.853(0.432-1.685)	0.647
MPV(references 7.4–11.0 fL)	7.4-11	Ref.	
	< 7.4	0.404(0.181-0.905)	0.028
	> 11	0.567(0.074-4.356)	0.585
PCT(references 0.16–0.43%)	0.16-0.43	Ref.	
	< 0.16	0.598(0.298-1.202)	0.149
	> 0.43		0.985
PDW(references 12.0–18.1%)	12-18.1	Ref.	
	< 12	0.668(0.28-1.596)	0.364
	> 18.1	2.82(0.904-8.797)	0.074
PT	CV	0.911(0.754-1.101)	0.336
PTA	CV	1.004(0.99-1.019)	0.553
INR	CV	0.298(0.034-2.606)	0.274
APTT(references 28–42 S)	CV	0.949(0.882-1.021)	0.160
APTT-R(references 28–42 S)	CV	0.093(0.008-1.064)	0.056
TT(references 28–42 S)	CV	1.109(0.987-1.245)	0.082
FIB(references 28–42 S)	CV	0.855(0.704-1.038)	0.113
ATⅢ(references 28–42 S)	CV	1.01(0.995-1.024)	0.208
D-Dimer(> 2.26 mg/L)	CV	1(0.966-1.035)	0.986
FDP	CV	1.006(0.999-1.013)	0.105
TT-R	CV	5.408(0.865-33.79)	0.071

649 Comparison of preoperative laboratory indicators between the two groups of patients. TP - total protein, ALB -
650 albumin, GLOB - globulin, A/G value (albumin/globulin), ALT - alanine aminotransferase, AST - aspartate
651 aminotransferase, TBIL - total bilirubin, DBIL - direct bilirubin, IBIL - indirect bilirubin, ALP - alkaline
652 phosphatase, GGT - γ-glutamyl transpeptidase, CHE - phenol red enzyme, TBA - total bile acid, HCRP - high-

sensitivity C-reactive protein, LDH - lactate dehydrogenase, CREA - creatinine, UA - uric acid, CA - calcium, P - phosphorus, Mg - magnesium, BNP - brain natriuretic peptide, WBC - white blood cells, NEUT - neutrophils, LYM - lymphocytes, MON - monocytes, EOS - eosinophils, BAS - basophils, RBC - red blood cells. Reference range: for females, 3.5–5.0 × 10^12/L; for males, 4.0–5.5 × 10^12/L. HGB - hemoglobin, reference range: for females, 110–150 g/L; for males, 120–160 g/L. HCT - hematocrit, 40–50%, MCV - mean cell volume, MCH - mean corpuscular hemoglobin content, MCHC - mean corpuscular hemoglobin concentration, RDW - red cell distribution width, PLT - platelets, 100–300 × 10^9/L, MPV - mean platelet volume. Platelet volume, PCT (procalcitonin), PDW (platelet distribution width), PT (prothrombin time), PTA (prothrombin activity), INR (international normalized ratio), APTT (activated partial thromboplastin time), APTT-R (ratio of activated partial thromboplastin time), TT (thrombin time), TT-R (thrombin ratio), FIB (fibrinogen), ATIII (antithrombin 3).

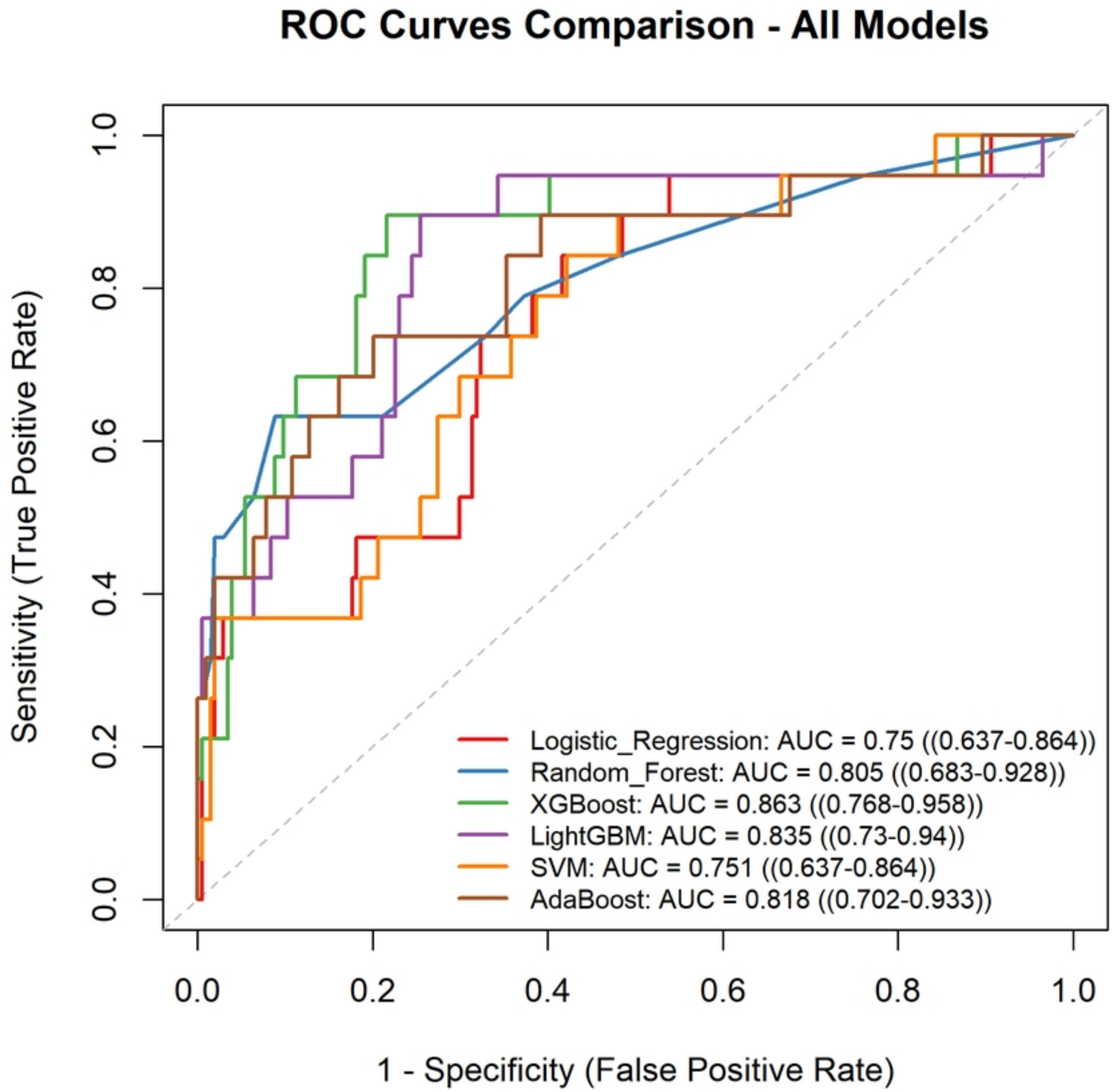
ROC Curves Comparison - All Models
Sensitivity (True Positive Rate)
1 - Specificity (False Positive Rate)
0.0
0.2
0.4
0.6
0.8
1.0
Logistic_Regression: AUC = 0.75 ((0.637-0.864))
Random_Forest: AUC = 0.805 ((0.683-0.928))
XGBoost: AUC = 0.863 ((0.768-0.958))
LightGBM: AUC = 0.835 ((0.73-0.94))
SVM: AUC = 0.751 ((0.637-0.864))
AdaBoost: AUC = 0.818 ((0.702-0.933))

Figure

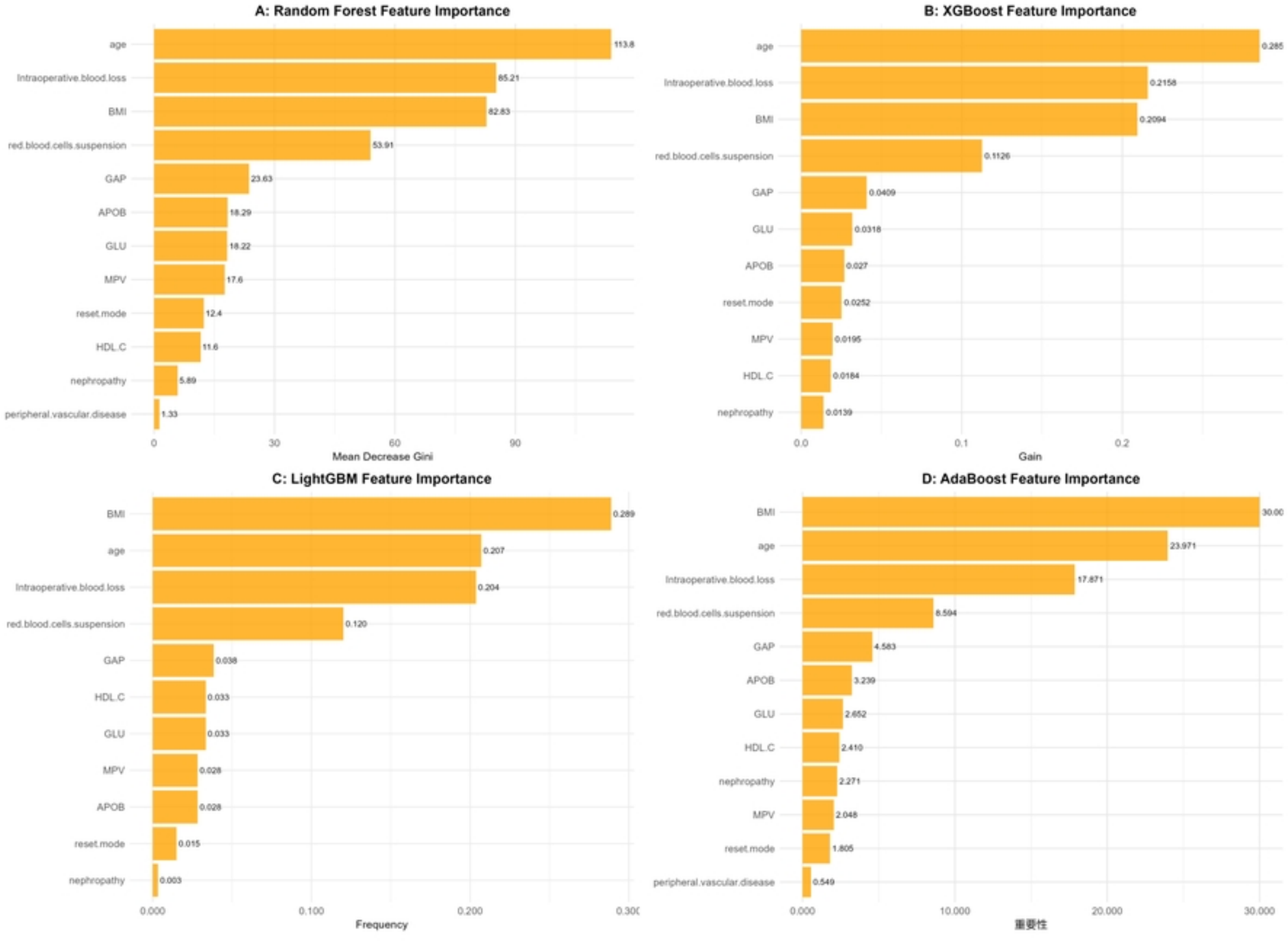
A: Random Forest Feature Importance
age
Intraoperative.blood.loss
BMI
red.blood.cells.suspension
GAP
APOB
GLU
MPV
reset.mode
HDL.C
nephropathy
peripheral.vascular.disease
113.8
85.21
82.83
53.91
23.63
18.29
18.22
17.6
12.4
11.6
5.89
1.33
0
30
60
90
Mean Decrease Gini
B: XGBoost Feature Importance
age
Intraoperative.blood.loss
BMI
red.blood.cells.suspension
GAP
GLU
APOB
reset.mode
MPV
HDL.C
nephropathy
0.285
0.2158
0.2094
0.1126
0.0409
0.0318
0.027
0.0252
0.0195
0.0184
0.0139
0.0
0.1
0.2
Gain
C: LightGBM Feature Importance
BMI
age
Intraoperative.blood.loss
red.blood.cells.suspension
GAP
HDL.C
GLU
MPV
APOB
reset.mode
nephropathy
0.289
0.207
0.204
0.120
0.038
0.033
0.033
0.028
0.028
0.015
0.003
0.000
0.100
0.200
Frequency
D: AdaBoost Feature Importance
BMI
age
Intraoperative.blood.loss
red.blood.cells.suspension
GAP
APOB
GLU
HDL.C
nephropathy
MPV
reset.mode
peripheral.vascular.disease
23.971
17.871
8.594
4.583
3.239
2.652
2.410
2.271
2.048
1.805
0.549
0.000
10.000
20.000
30.000
重要性

Figure

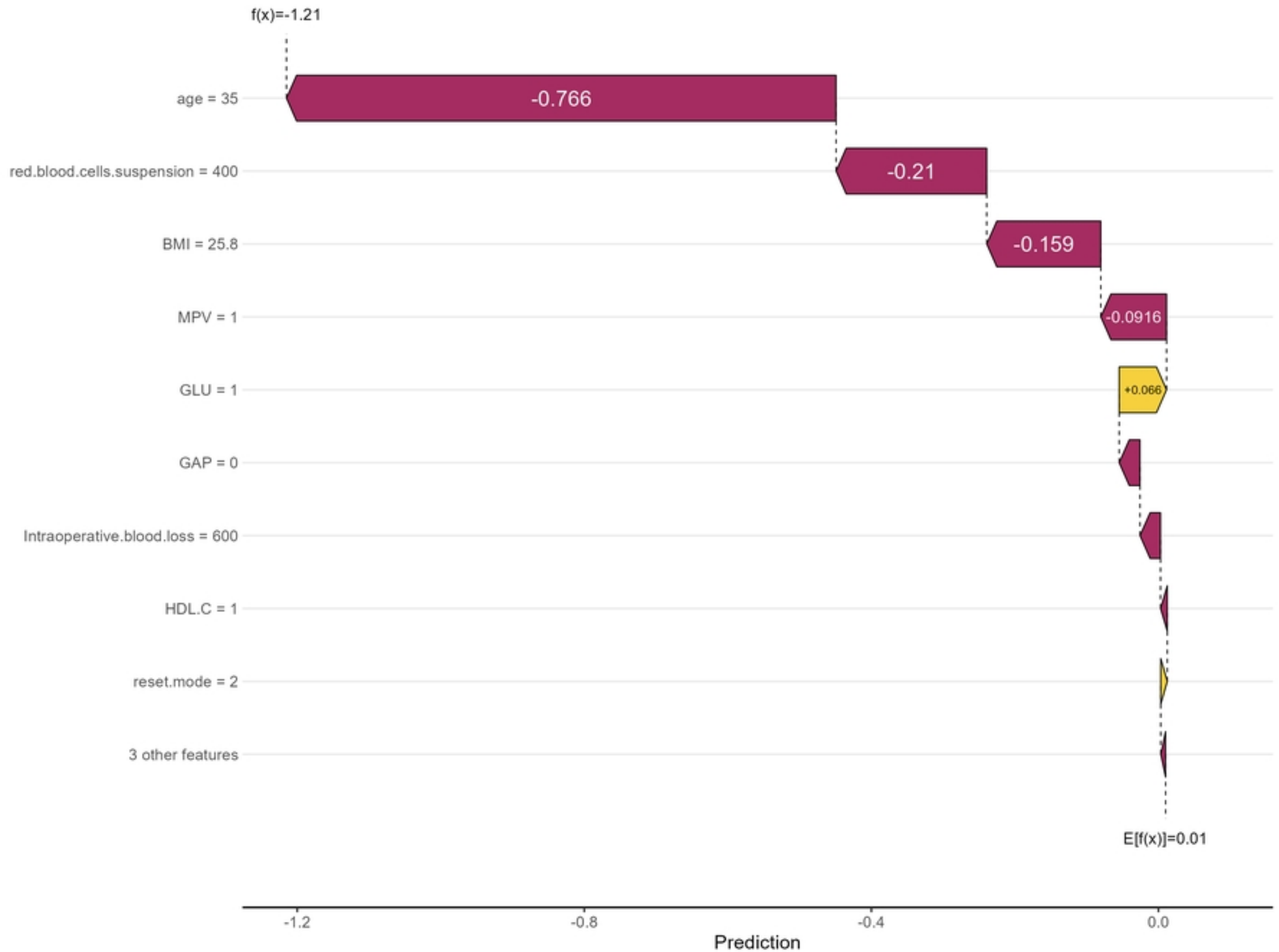
f(x)=-1.21
age = 35
-0.766
red.blood.cells.suspension = 400
-0.21
BMI = 25.8
-0.159
MPV = 1
-0.0916
GLU = 1
+0.066
GAP = 0
Intraoperative.blood.loss = 600
HDL.C = 1
reset.mode = 2
3 other features
E[f(x)]=0.01
-1.2
-0.8
-0.4
0.0
Prediction

Figure

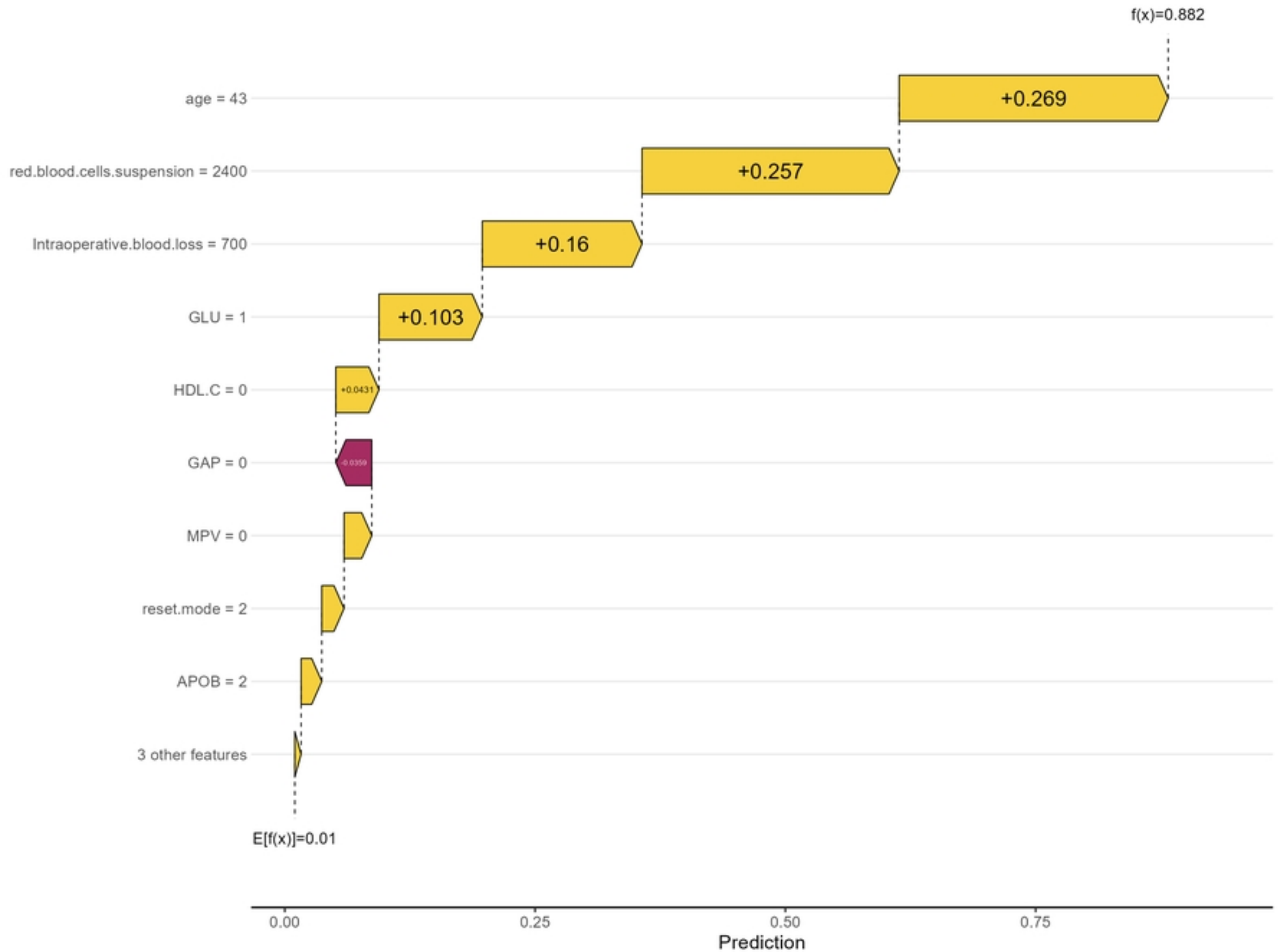
f(x)=0.882
age = 43
+0.269
red.blood.cells.suspension = 2400
+0.257
Intraoperative.blood.loss = 700
+0.16
GLU = 1
+0.103
HDL.C = 0
+0.0431
GAP = 0
-0.0359
MPV = 0
reset.mode = 2
APOB = 2
3 other features
E[f(x)]=0.01
0.00
0.25
0.50
0.75
Prediction

Figure

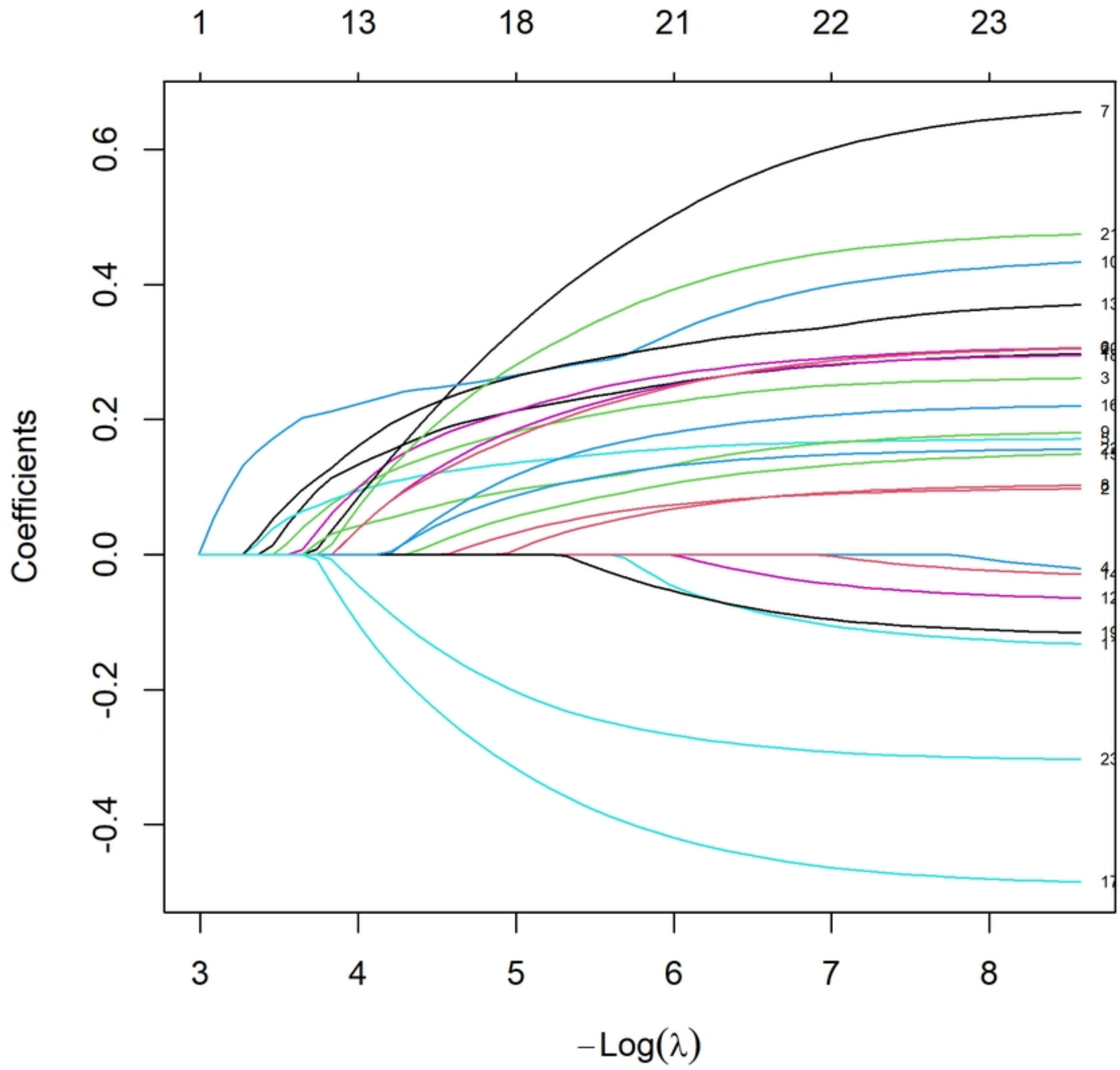
1
13
18
21
22
23
Coefficients
0.6
0.4
0.2
0.0
-0.2
-0.4
7
21
10
13
3
16
4
12
23
17
3
4
5
6
7
8
−Log(λ)

Figure

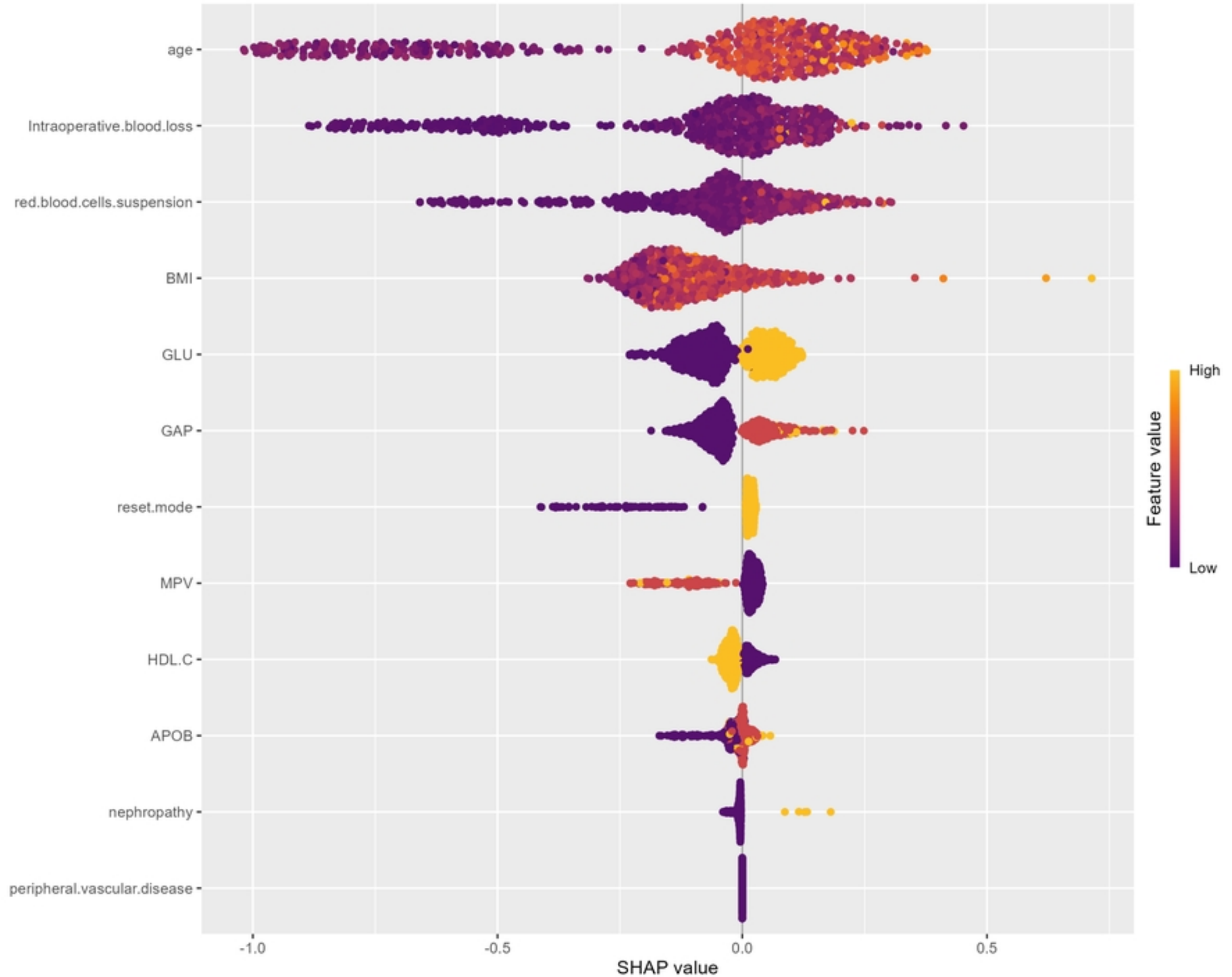
age
Intraoperative.blood.loss
red.blood.cells.suspension
BMI
GLU
GAP
reset.mode
MPV
HDL.C
APOB
nephropathy
peripheral.vascular.disease
-1.0
-0.5
0.0
0.5
SHAP value
High
Feature value
Low

Figure

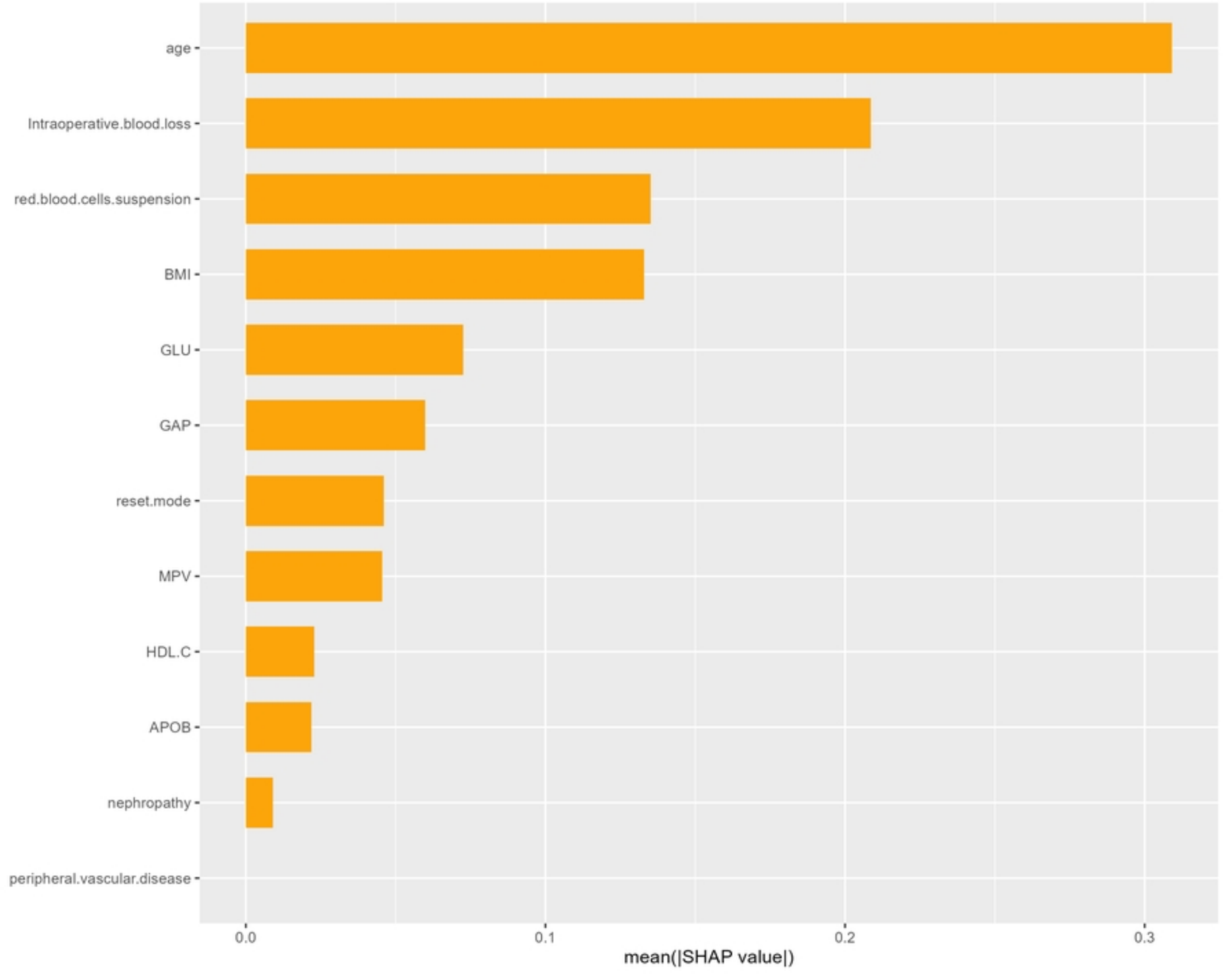
age
Intraoperative.blood.loss
red.blood.cells.suspension
BMI
GLU
GAP
reset.mode
MPV
HDL.C
APOB
nephropathy
peripheral.vascular.disease
0.0
0.1
0.2
0.3
mean(|SHAP value|)

Figure

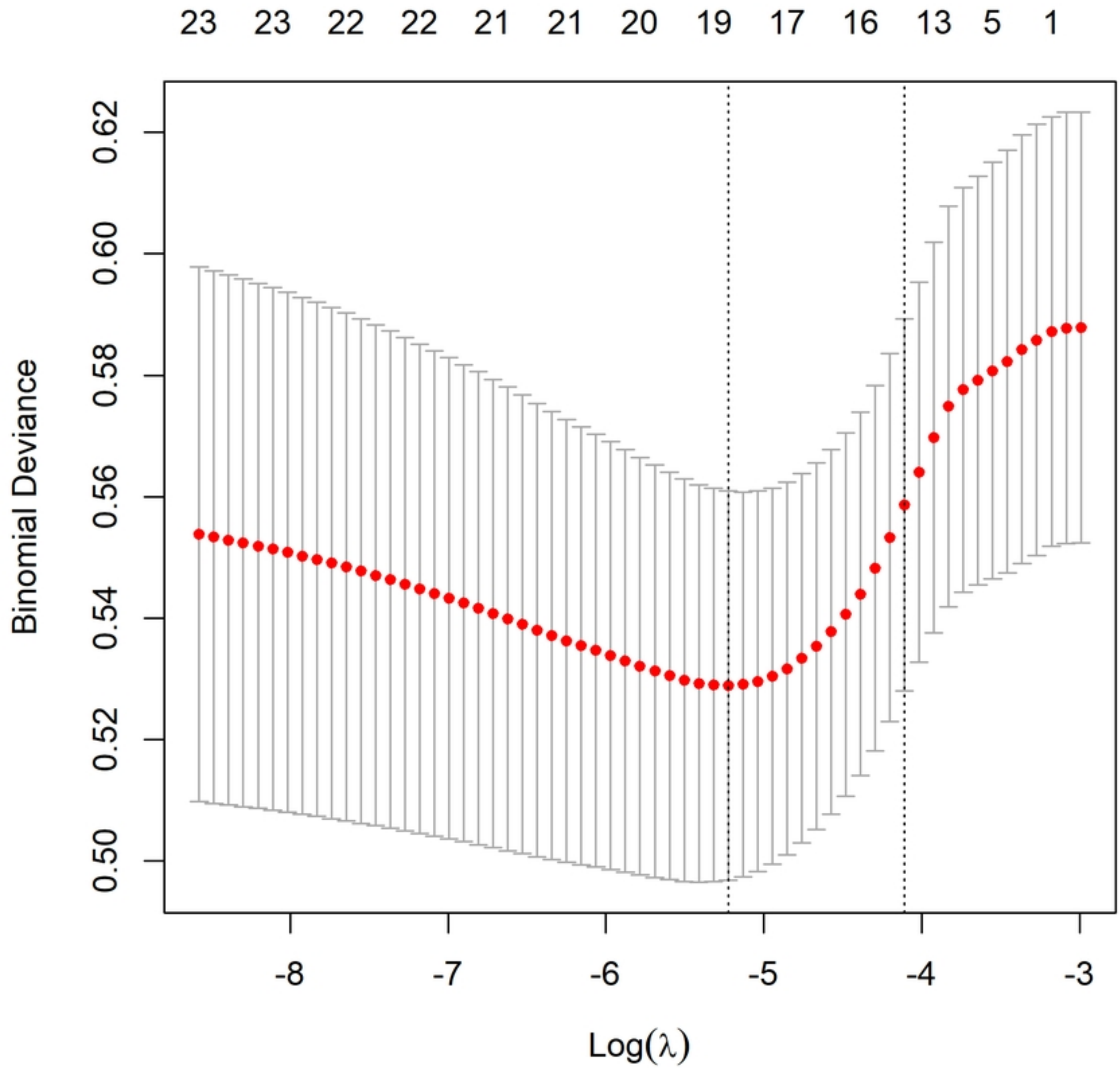
23 23 22 22 21 21 20 19 17 16 13 5 1
Binomial Deviance
0.50
0.52
0.54
0.56
0.58
0.60
0.62
-8
-7
-6
-5
-4
-3
Log(λ)

Figure